NUSOD 2021

Design and Simulation of C-Shaped Optical Fiber Sensor

N. M. Razali, S. Ambran*, S. N. F. Zuikafly, M. A. M. Yuzir, H. H .J. Sapingi
Malaysia – Japan International Institute of Technology
Universiti Teknologi Malaysia
Kuala Lumpur, Malaysia
*sumiaty.kl@utm.my

***Abstract*—This paper presents a C-shaped optical fiber sensor for refractive index measurement. The design and simulation of the C-shaped optical fiber were conducted via Wave Optics Module-COMSOL Multiphysics®. The refractive index measurement ranging from 1.30-1.40 is performed. The simulation results showed that the C-shaped design has the potential to act as a refractive index sensor with sensitivity of up to 0.966348101, higher than simulated D-shaped OFS with estimated sensitivity of up to 0.966334412.**

Keywords*—*design, simulation, C - shaped, optical fiber sensor, refractive index

I. Introduction

Optical fiber sensor (OFS), a well-known refractometer has been widely demonstrated in measuring physical, chemical, and biological parameters, offering simple refractive index (RI) measurement for quality control and in situ monitoring. To fabricate this optical miniature sensor, a part of the optical fibre cladding is modified and replaced with target measurand either in form of liquid, gas, or vapour to measure its various properties based on the RI changes. Microfiber OFS has strong sensitivity performance in which the cladding layer is fully modified to expose the evanescent field to interact with the sensing medium. However, after cladding modification, a small segment of the fiber becomes extremely thin, causing it to be fragile and hard to handle [1, 2]. To mitigate these drawbacks, side-polished OFS has been introduced where the one side of the fibre is polished to form a D-shaped structure. Despite the heightened mechanical stability from the cladding support as compared to the microfiber OFS, it has low sensitivity due to limited evanescent field exposure [3].

An early investigation of the C-shaped OFS was conducted by Tan et al. in which the C-shaped design was implemented on fiber Bragg grating to act as a temperature-insensitive refractometer with similar operating principle as the D-shaped OFS [4]. The C-shaped structure offers strong mechanical stability to support the sensor and greater evanescent wave exposure compared to D-shaped OFS. In another work, Xie et al. used dual C-shaped cavities to develop a Fabry-Perot interferometer (FPI) based sensor [5]. The C-shaped cavities consist of an inner bore diameter of 40 µm and an outer diameter of 160 µm which were serially spliced to the SMF in alternate arrangement. The proposed sensor showed its strong potential for highly stable sensing application in measuring biological samples. Additionally, the sensor can be fabricated on-tower and multiplexed.

Despite the limited available literature on this particular sensor design, its advantages as mentioned before have proven its feasibility as a new OFS design. In this paper, a C-shaped OFS is designed and simulated via Wave Optics Module-COMSOL Multiphysics® software. Furthermore, the electric field distribution throughout the sensor and effective RI changes at different analyte RI medium are also studied and the underlying physics are discussed.

II. Design and Simulation

The 3-dimensional and cross section of the structure under investigation are illustrated in Fig. 1. The structure consists of single mode fiber (SMF) with core and cladding diameter of 8µm and 125µm, respectively. As depicted in Fig. 1(a), to form the 'C' shape, a quarter of the cladding structure was cut-off using right triangle at apex of 90° from the fibre centre. The cut-off region was then replaced with sensing medium (analyte) for simulation purposes as shown in Fig. 1(b). 1550nm is chosen as the operating wavelength where the lowest attenuation window of practical fiber is established [6]. The analyte RI is set from 1.30-1.40, the typical range of a liquid RI [7]. A three-term Sellmeier equation is used to express the SMF's RI at near infrared wavelength region as described in Eq. 1:

$$n^2 - 1 = \frac{A_1\lambda^2}{\lambda^2 - \lambda_1^2} + \frac{A_2\lambda^2}{\lambda^2 - \lambda_2^2} + \frac{A_1\lambda^2}{\lambda^2 - \lambda_3^2} \quad (1)$$

Where, n is the refractive index of the material and λ is the operating wavelength. Both core and cladding have different Sellmeier coefficients. Detail information can be found in this reference [8].

III. Results and Discussion

A. Electric Field Disctribution

Fig. 2 shows the simulation output as the light wave propagates through the fibre structure. In a selective study, the coloured illustration of the electric field distribution is illustrated through SMF and C-shaped optical fiber when exposed to the analyte medium at 1.33 of RI for comparison purposes as shown in Fig. 2(a) and Fig. 2(b). The red and blue colour represents the maximum and the minimum electric field intensity. In the SMF structure, the electric field is concentrated at the centre and equally distributed indicating that the light is strongly confined in the core. In contrast, in the C-shaped sensor, the electric field slightly shifted towards the core/cladding boundary due to lower RI contrast between these two mediums compared to core/analyte boundary. For both cases, the electric field gradually decreases when

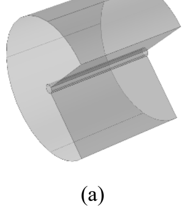

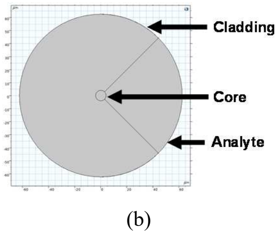

(a) (b)

Fig. 1. The structure of C – shaped OFS in a) 3D and b) cross section geometry for simulation purposes

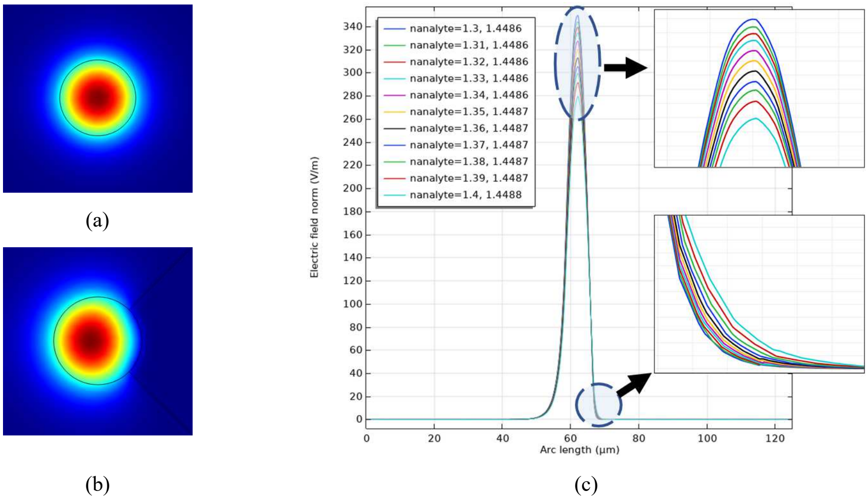

Fig. 2. Coloured illustration of normalized electric field intensity around the fiber core for (a) SMF, (b) C – shaped when exposed to the analyte medium with RI of 1.33 and (c) MFD of C – shaped OFS at different analye RI

reaching the core/ cladding and core/analyte boundary as the light energy attenuated as it reaches the boundary with different RI medium. The electric field distribution of the C-shaped OFS can be analysed by studying the mode field diameter (MFD) as depicted in Fig. 2(c). A large variation of MFD can be seen by changing the analyte RI. At the core/analyte boundary, the penetration depth of the evanescent wave increases with the increase in analyte RI. The penetration depth depends on the RI difference between the core and the analyte. The lower the RI difference, the higher the penetration depth probing further into the analyte medium which in turn leads to more energy dissipation, hence, decreasing the electric field intensity.

B. Effective Refractive Index and Sensor Sensitivity

Effective RI, n_{eff} refers to the effective property of the waveguide altogether with given measurand. In principle, the n_{eff} is not influenced by external surrounding medium but the cladding modification can significantly affect the n_{eff} of the waveguide due to evanescent wave interaction while counting the analyte medium as a part of its n_{eff} value. Different n_{eff} can be obtained by changing the analyte RI. The registered n_{eff} changes are plotted at different analyte RI as shown in Fig. 3. As the analyte RI increases from 1.30 to 1.40, the n_{eff} also increases. The estimated sensitivity achieved by the C-shaped OFS is 0.966348101, higher than simulated closest design, D-shaped OFS, with estimated sensitivity of 0.966334412 which

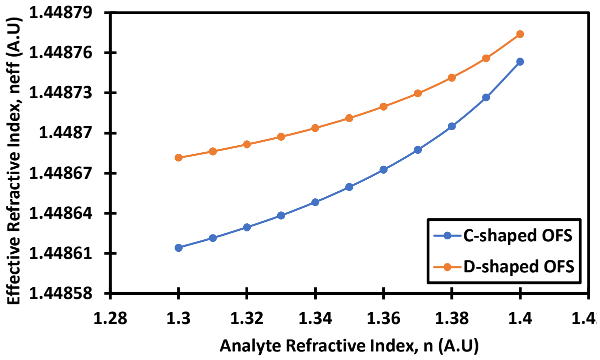

Fig. 3. Effective RI changes of C – shaped and D - shaped OFS at different analyte RI

results at the highest analyte RI of 1.40. This is expected since the evanescent wave exposure area of C-shaped is larger than D-shaped OFS.

IV. Conclusion

This work demonstrated the design and simulation of C-shaped OFS at different refractive index ranging from 1.30-1.40. Different analyte RI shows different electric field distribution and evanescent field without being overlapped. The estimated sensitivity achieved by the C-shaped sensor is 0.966348101, higher than simulated D-shaped OFS with estimated sensitivity of 0.966334412 which results at the highest analyte RI of 1.40. The simulated design pointed to a convincing potential design as a new type of OFS.

Acknowledgment

The project is financially supported by AUN/SEED-Net Grant with Vote No. R.K130000.7343.4B616.

References

[1] G Patil, J.J., Y.H. Patil, and A. Ghosh. *Comprehensive and Analytical Review on Optical Fiber Refractive Index Sensor*. in *2020 4th International Conference on Trends in Electronics and Informatics (ICOEI)(48184)*. 2020.

[2] Zhao, Y., et al., *Applications of fiber-optic biochemical sensor in microfluidic chips: A review*. Biosens Bioelectron, 2020. **166**: p. 112447.

[3] J. Dudus, A., R. Blue, and D. Uttamchandani, *Comparative Study of Microfiber and Side-Polished Optical Fiber Sensors for Refractometry in Microfluidics*. IEEE Sensors Journal, 2013. **13**(5): p. 1594-1601.

[4] Tan, R.X., et al., *Birefringent Bragg Grating in C-Shaped Optical Fiber as a Temperature-Insensitive Refractometer*. Sensors, 2018. **18**(10): p. 3285.

[5] Xie, L.S., et al., *Multiplexed Optical Fiber Biochemical Sensing Using Cascaded C-Shaped Fabry-Perot Interferometers*. Ieee Sensors Journal, 2019. **19**(22): p. 10425-10431.

[6] R. Nicole, Green, L.D., *Fiber Optic Communications*. 2019: CRC Press.

[7] Chen, C., et al., *Compact refractive index sensor based on an S-tapered fiber probe*. Optical Materials Express, 2018. **8**(4): p. 919-925.

[8] Oh, K. and U.-C. Paek, *Silica Optical Fiber Technology for Devices and Components: Design, Fabrication, and International Standards*. Vol. 240. 2012: John Wiley & Sons.